INTERFACE FOCUS

royalsocietypublishing.org/journal/rsfs

Research

Cite this article: Clarke VC, Danila FR, von Caemmerer S. 2021 CO_2 diffusion in tobacco: a link between mesophyll conductance and leaf anatomy. *Interface Focus* **11**: 20200040. https://doi.org/10.1098/rsfs.2020.0040

Accepted: 9 December 2020

One contribution of 13 to a theme issue 'Carbon dioxide detection in biological systems'.

Subject Areas:
biochemistry

Keywords:
CO_2 diffusion, carbon isotope discrimination, cell wall, image analysis, leaf anatomy, leaf age

Author for correspondence:
Victoria C. Clarke
e-mail: tory.clarke@anu.edu.au

Electronic supplementary material is available online at https://doi.org/10.6084/m9.figshare.c.5271262.

THE ROYAL SOCIETY PUBLISHING

CO_2 diffusion in tobacco: a link between mesophyll conductance and leaf anatomy

Victoria C. Clarke, Florence R. Danila and Susanne von Caemmerer

Australian Research Council Centre of Excellence for Translational Photosynthesis, Division of Plant Science, Research School of Biology, The Australian National University, Acton, Australian Capital Territory 2601, Australia

VCC, 0000-0002-1028-6749; FRD, 0000-0002-7352-3852; SvC, 0000-0002-8366-2071

The partial pressure of CO_2 at the sites of carboxylation within chloroplasts depends on the conductance to CO_2 diffusion from intercellular airspace to the sites of carboxylation, termed mesophyll conductance (g_m). We investigated how g_m varies with leaf age and through a tobacco (*Nicotiana tabacum*) canopy by combining gas exchange and carbon isotope measurements using tunable diode laser spectroscopy. We combined these measurements with the anatomical characterization of leaves. CO_2 assimilation rate, A, and g_m decreased as leaves aged and moved lower in the canopy and were linearly correlated. This was accompanied by large anatomical changes including an increase in leaf thickness. Chloroplast surface area exposed to the intercellular airspace per unit leaf area (S_c) also decreased lower in the canopy. Older leaves had thicker mesophyll cell walls and g_m was inversely proportional to cell wall thickness. We conclude that reduced g_m of older leaves lower in the canopy was associated with a reduction in S_c and a thickening of mesophyll cell walls.

1. Introduction

In plants with the C_3 photosynthetic pathway, mesophyll conductance, g_m, quantifies the ease with which CO_2 diffuses from intercellular airspace within a leaf to the sites of Rubisco carboxylation within chloroplasts [1,2]. It is one of the three main physiological processes limiting CO_2 uptake and fixation, the others being CO_2 diffusion from the atmosphere to the sub-stomatal cavity (stomatal conductance, g_s) and the biochemical activity of Rubisco and RuBP regeneration. Studies have shown that global crop production needs to double by 2050 to meet the projected demands from a rising population, diet shifts and increasing biofuels consumption [3]. The need to understand and maximize g_m is part of the research efforts being made to enhance photosynthesis to improve crop yield. For example, enhancements of photosynthesis through manipulation of chloroplast function will be diminished through the reduction in chloroplast CO_2 partial pressure unless it is combined with improved g_m [4–9]. Increasingly, crop models are incorporating leaf and canopy level parameters to better predict where photosynthesis improvements can be made (e.g. [10]), and an understanding of mesophyll conductance variation across leaf positions is crucial for this.

At present, there is an incomplete mechanistic understanding of g_m (see Cousins *et al.* [11] for a review of recent developments in g_m in C_3 and C_4 species). To enhance CO_2 diffusion, chloroplasts are spread thinly along cell wall surfaces, and their surface area appressing intercellular airspace is up to 20 times leaf surface area and good correlation between g_m and S_c (chloroplast surface area exposed to the intercellular airspace per unit leaf area) has been observed [12–14]. However, across species, this correlation is not unique and mesophyll cell wall thickness and its porosity, as well as membrane permeability to CO_2 and liquid diffusion, are also considered important

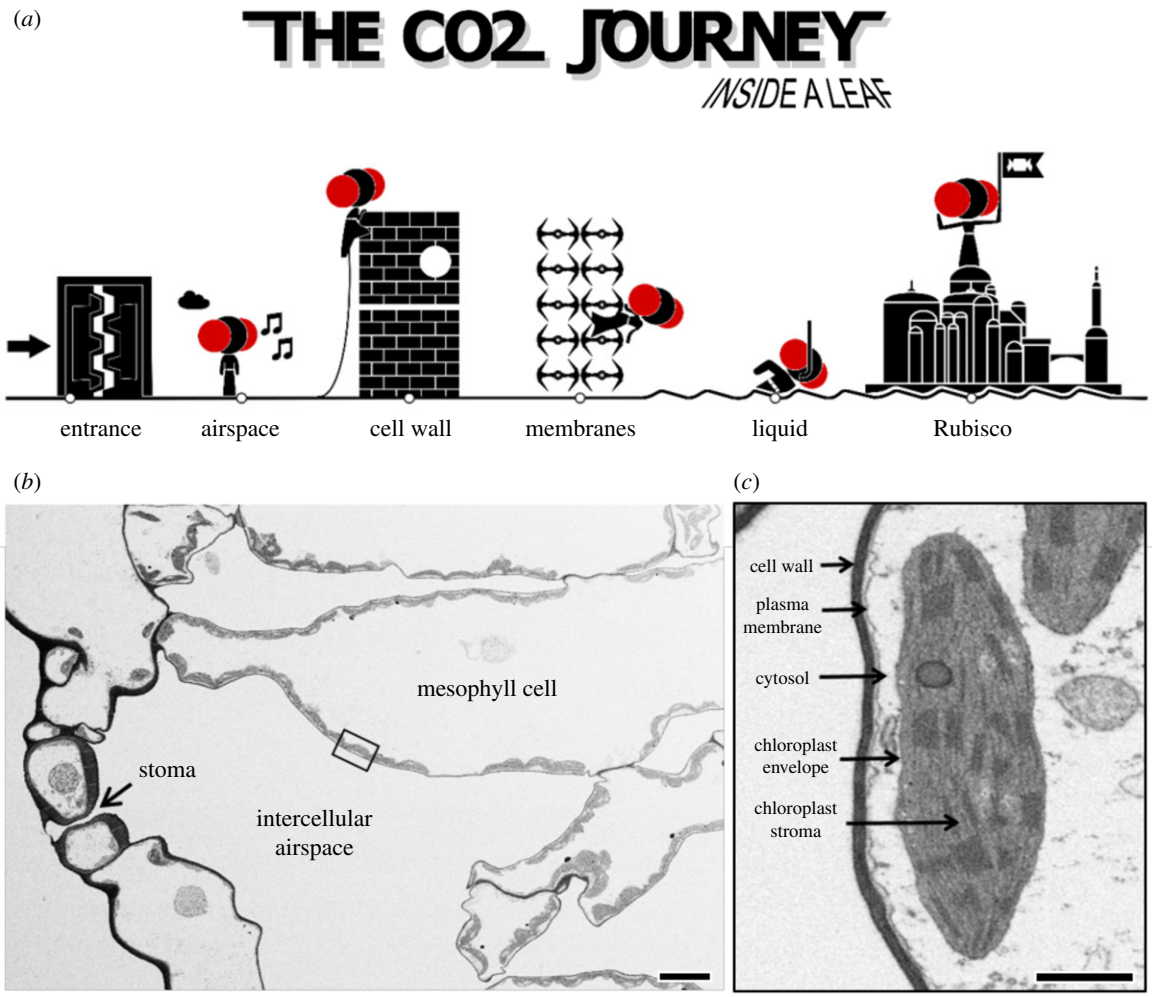

Figure 1. A Star Wars-inspired cartoon depicting the CO_2 diffusion journey inside the leaf with Princess Leia representing a CO_2 molecule (*a*) and the corresponding electron micrographs illustrating the actual CO_2 diffusion pathway within a tobacco leaf (*b* and *c*). For photosynthetic CO_2 assimilation to occur, CO_2 has to diffuse through stomata (entrance), intercellular airspace, cell wall, membranes (plasma membrane and chloroplast envelope) and the liquid phase in the cytosol and chloroplast stroma. Once inside the chloroplast, CO_2 is then fixed by Rubisco into energy-rich sugars as part of the photosynthesis process. Bar in $b = 10$ µm; bar in $c = 1$ µm.

parameters of g_m [12,14,15]. Figure 1 outlines the CO_2 diffusion path within the leaf.

There have been a number of studies that have examined variation in g_m with leaf age in tree species [14,16–18] but fewer studies have looked at variation in g_m with leaf age in crop species [19–21]. Here, we have examined the changes in CO_2 assimilation rate and g_m with leaf age and canopy position in tobacco to assess the linkage between g_m and leaf anatomy, and provide information on how best to model variation in g_m in a C_3 crop canopy.

2. Material and methods

2.1. Plant growth

Tobacco (*Nicotiana tabacum*, L. cv Samsun) was grown in a naturally lit glasshouse with day/night temperatures set at 28/18°C. Seeds were sown in the glasshouse in commercial seed raising mix, then transferred after two weeks to 5 l pots filled with commercial potting mix supplemented with slow-release fertilizer (Osmocote Exact, Scotts, NSW, Australia). Plants were grown in Canberra, Australia between June and August 2019, with an average day length of 10 h. Average light intensity at midday during the growing period was 700 µmol m^{-2} s^{-1}. Plants were watered daily.

2.2. Concurrent measurements of gas exchange and carbon isotope discrimination to quantify mesophyll conductance

Gas exchange and carbon isotope discrimination measurements were made as described by Tazoe *et al.* [22] using a 6 cm^2 chamber of the LI-6400 with a red–blue light-emitting diode (LED) light source (Li-Cor, Lincoln, NE, USA). Two LI-6400 chambers and the plants were placed in a temperature-controlled cabinet with fluorescent lights (TRIL1175, Thermoline Scientific Equipment, Smithfield, NSW 2164, Australia). The CO_2 in the leaf chamber was set at 380 µmol mol^{-1}, flow rate at 200 µmol s^{-1} and irradiance at 1500 µmol quanta m^{-2} s^{-1}. Leaf temperature was controlled at 25°C. Two percent of O_2 in N_2, mixed by mass flow controllers (Omega Engineering Inc, Stamford, CT, USA), was supplied to the LI-6400s after humidification of the air by adjusting the temperature of the water circulating around a Nafion tube (Perma Pure LLC, Toms River, NJ, USA, MH-110-12P-4). Gas exchange was coupled to a tunable diode laser (TDL; TGA100a, Campbell Scientific, Inc., Logan, UT, USA) for concurrent measurements of carbon isotope composition. Measurements were made at 4 min intervals for 20 s, with 10–12 measurements per leaf and the last five measurements were averaged. The $\delta^{13}C$ of CO_2 gas cylinders ($\delta^{13}C_{tank}$) used in the LI-6400 CO_2 injector system was 14‰. Gas exchange was calculated using the equations presented by von Caemmerer and Farquhar [23]

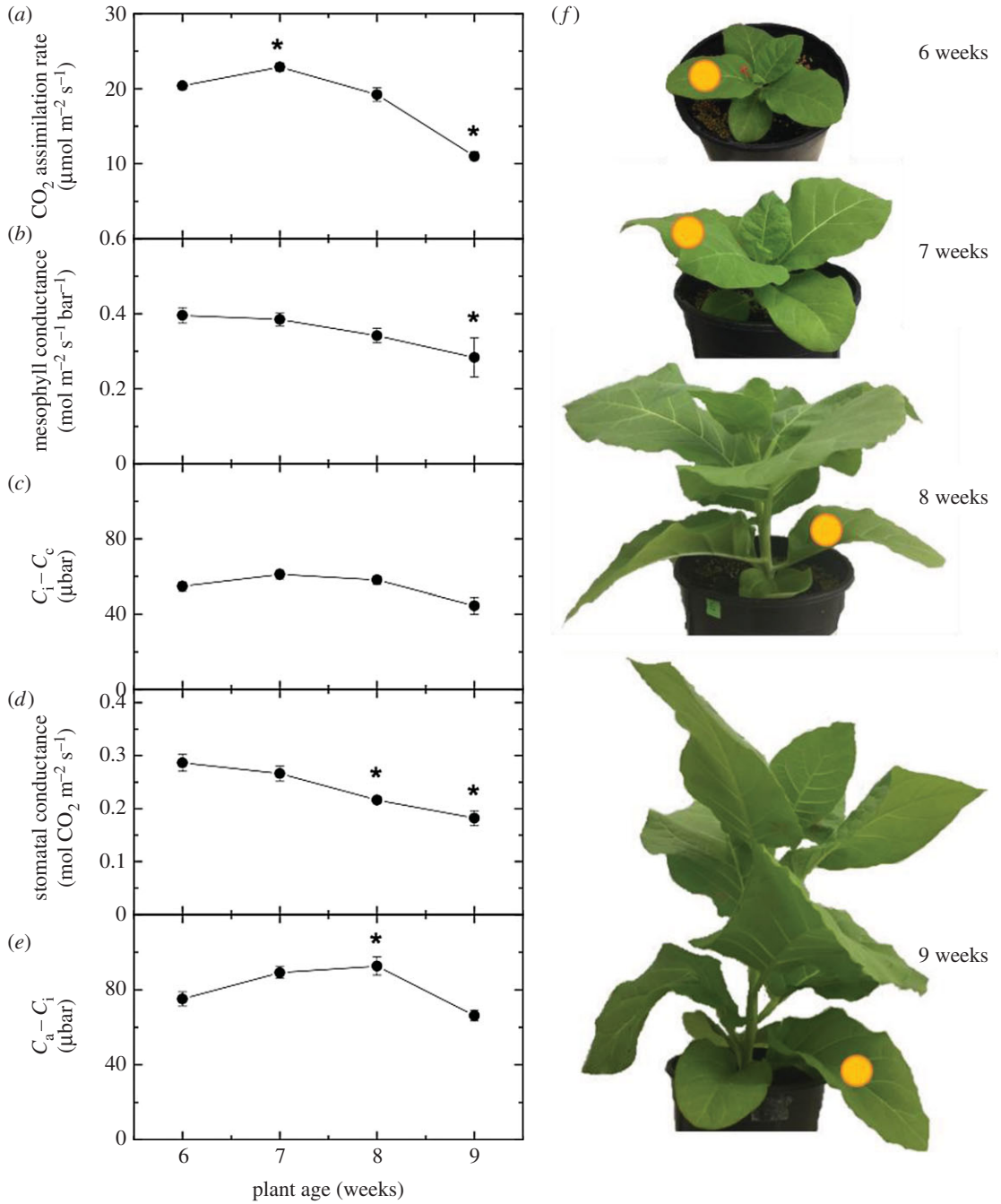

Figure 2. Variation in CO_2 assimilation rate, mesophyll conductance, $C_i - C_c$, stomatal conductance and $C_a - C_i$ over time with increasing leaf age. Gas exchange measurements were made at an irradiance of 1500 µmol m^{-2} s^{-1}, ambient CO_2 of 380 µbar, 2% O_2 and a leaf temperature of 25°C. Gas exchange measurements were made concurrently with measurements of carbon isotope discrimination using tunable diode laser spectroscopy for the calculation of mesophyll conductance (see Materials and methods), $n = 4$. Timepoints significantly different from 6-week-old plants are indicated with an asterisk. The same leaves were followed over time, and measured leaf is denoted with a yellow circle on plant images. Raw data are given in the electronic supplementary material, Data File S1.

and Δ was calculated from the equation presented by Evans *et al.* [24]. Values of $\xi = C_{ref}/(C_{ref} - C_{sam})$ ranged between 4 and 14, where C_{ref} and C_{sam} are the CO_2 concentrations of dry air entering and exiting the leaf chamber, respectively, measured by the TDL. Measurements were taken on four 6- to 9-week-old plants with 3–12 leaves. Mesophyll conductance, g_m, was calculated as described by Evans & von Caemmerer [25].

2.3. Biochemical measurements of Rubisco site content and leaf nitrogen

Total Rubisco content was estimated from leaf discs by the irreversible binding of [^{14}C]2-carboxy-D-arabinitol 1,5-bisphosphate to the fully carbamylated enzyme as described by Ruuska *et al.* [26]. Leaf nitrogen (N) was determined on leaf discs which were oven-dried at 80°C, weighed and then ground to powder. Percentage of N was determined on the ground tissues using a flash combustion CNS analyser (Fison NA1500; Fison Instruments, Milan, Italy).

2.4. Anatomical measurements

Leaf anatomy was determined from light and scanning electron micrographs of transverse sections of resin-embedded leaf tissue collected from leaf positions 1 to 10 of three 9-week-old tobacco plants (figure 3). Leaf tissue was collected from the same area used for the concurrent gas exchange and carbon isotope discrimination measurement and immediately processed for light and electron microscopy as previously described [27]. Light micrographs were obtained using a Leica DM5500 compound

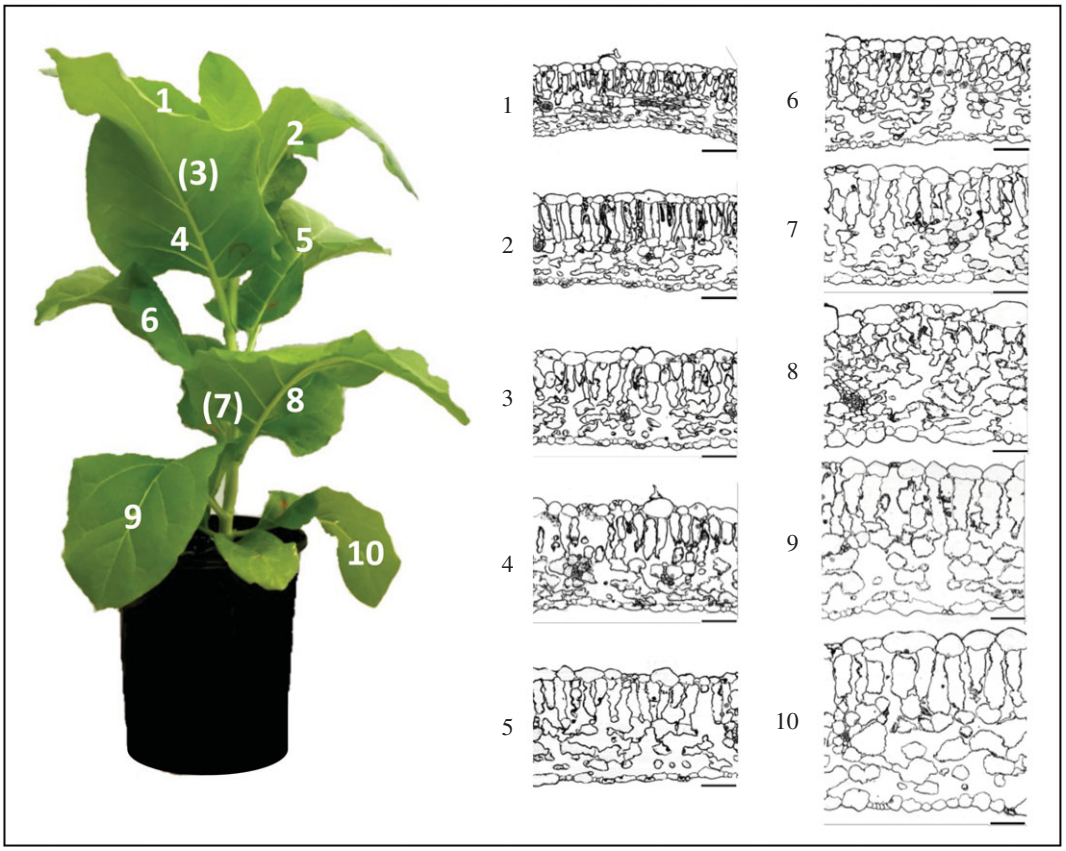

Figure 3. Light micrographs of transverse sections of resin-embedded leaf tissue collected from leaf position 1 to 10 of 9-week-old tobacco plant showing variation in leaf thickness (see figure 5*b* for measured values). Bars = 100 µm.

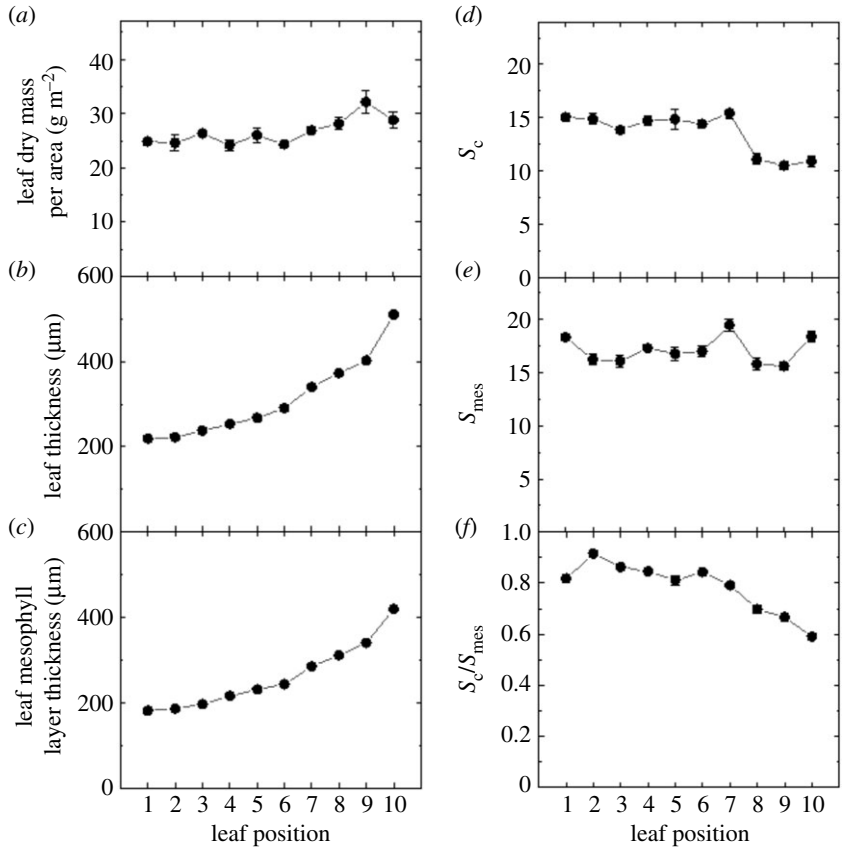

Figure 4. Variation in leaf dry mass per area (LMA, $n = 4$ plants) (*a*), leaf thickness (*b*), leaf mesophyll layer thickness (*c*), S_c, chloroplast surface area exposed to intercellular airspace per unit leaf area (*d*), S_{mes}, mesophyll surface area exposed to intercellular airspace per unit leaf area (*e*), and S_c/S_{mes} (*f*) with leaf position in the canopy (figure 3). For anatomical measurements, $n = 3$ plants. Raw data are given in the electronic supplementary material, Data File S2.

Table 1. Means comparison using Tukey test of the physiological and anatomical parameters measured between different leaf positions of tobacco plant. The number 1 denotes significant difference at $p < 0.05$ and 0 denotes no significant difference at $p < 0.05$.

leaves compared	A	$C_a - C_i$	$C_i - C_c$	g_m	g_s	stomatal density	leaf N	Rubisco sites	LMA	leaf thickness	leaf M layer thickness	S_c	S_{mes}	S_c/S_{mes}	chloroplast thickness	chloroplast length	cell wall thickness
2 1	0	0	0	0	0	0	0	0	0	0	0	0	0	1	1	0	0
3 1	0	0	0	0	0	0	0	0	0	0	1	0	1	0	1	0	1
3 2	0	0	0	0	0	0	0	0	0	0	1	0	0	0	0	0	1
4 1	0	0	0	0	0	0	0	0	0	1	1	0	0	0	1	0	1
4 2	0	0	0	0	0	0	0	0	0	1	1	0	0	1	0	0	1
4 3	0	0	0	0	0	0	0	0	0	0	1	0	0	0	0	0	0
5 1	0	0	0	0	0	1	1	0	0	1	1	0	0	0	1	0	0
5 2	0	0	0	0	0	1	0	0	0	1	1	0	0	1	0	0	0
5 3	0	0	0	0	0	1	1	1	0	1	1	0	0	0	0	0	1
5 4	0	0	0	0	0	0	0	0	0	0	1	0	0	0	0	0	1
6 1	0	0	0	0	1	1	1	1	0	1	1	0	0	0	1	1	1
6 2	0	0	0	0	1	1	1	1	0	1	1	0	0	1	1	0	1
6 3	0	0	0	0	1	1	1	1	0	1	1	0	0	0	1	1	0
6 4	0	0	0	0	1	1	0	0	0	1	1	0	0	0	1	1	0
6 5	0	0	0	0	0	0	0	0	0	0	1	0	0	0	1	1	1
7 1	1	0	0	0	1	1	1	1	0	1	1	0	0	0	1	0	1
7 2	1	0	0	0	1	1	1	1	0	1	1	0	1	1	0	0	1
7 3	1	0	0	0	1	1	1	1	0	1	1	0	1	1	0	0	1
7 4	1	0	0	0	1	1	1	0	0	1	1	0	1	1	0	0	1
7 5	1	0	0	1	1	1	0	0	0	1	1	0	1	0	0	0	1
7 6	1	0	0	0	0	0	0	0	0	1	1	0	1	0	1	1	1

(*Continued*.)

Table 1. (*Continued.*)

leaves compared	A	$C_a - C_i$	$C_i - C_c$	g_m	g_s	stomatal density	leaf N	Rubisco sites	LMA	leaf thickness	leaf M layer thickness	S_c	S_{mes}	S_c/S_{mes}	chloroplast thickness	chloroplast length	cell wall thickness
8 1	1	0	0	0	1	1	1	1	0	1	1	1	1	1	1	0	1
8 2	1	0	0	0	1	1	1	1	0	1	1	1	0	1	0	0	1
8 3	1	0	0	0	1	1	1	1	0	1	1	1	0	1	1	0	1
8 4	1	0	0	0	1	1	1	0	0	1	1	1	0	1	1	0	1
8 5	1	0	0	1	1	1	1	0	0	1	1	1	0	1	0	0	1
8 6	1	0	0	0	0	1	0	0	0	1	1	1	0	1	1	0	1
8 7	0	0	0	0	0	0	0	0	0	1	1	1	1	1	0	0	1
9 1	1	0	0	0	1	1	1	1	1	1	1	1	1	1	0	1	1
9 2	1	0	0	1	1	1	1	1	1	1	1	1	0	1	1	1	1
9 3	1	0	1	0	1	1	1	1	1	1	1	1	0	1	1	1	1
9 4	1	0	0	1	1	1	1	1	1	1	1	1	0	1	1	1	1
9 5	1	0	0	1	1	1	1	0	1	1	1	1	0	1	1	1	1
9 6	1	1	0	1	1	1	1	0	1	1	1	1	0	1	1	0	1
9 7	1	0	0	0	1	1	0	0	0	1	1	1	1	1	1	1	1
9 8	1	0	0	0	0	0	0	0	0	1	1	0	0	0	1	1	1
10 1	1	0	0	1	1	1	1	1	0	1	1	1	0	1	1	1	1
10 2	1	0	0	1	1	1	1	1	0	1	1	1	0	1	0	1	1
10 3	1	0	1	1	1	1	1	1	0	1	1	1	0	1	1	1	1
10 4	1	0	0	1	1	1	1	1	0	1	1	1	0	1	1	1	1
10 5	1	0	0	1	1	1	1	1	0	1	1	1	0	1	0	1	1
10 6	1	1	0	1	1	1	1	0	0	1	1	1	0	1	1	1	1
10 7	1	0	0	1	1	1	1	0	0	1	1	1	0	1	1	1	1
10 8	1	1	0	1	0	0	0	0	0	1	1	0	1	1	0	1	1

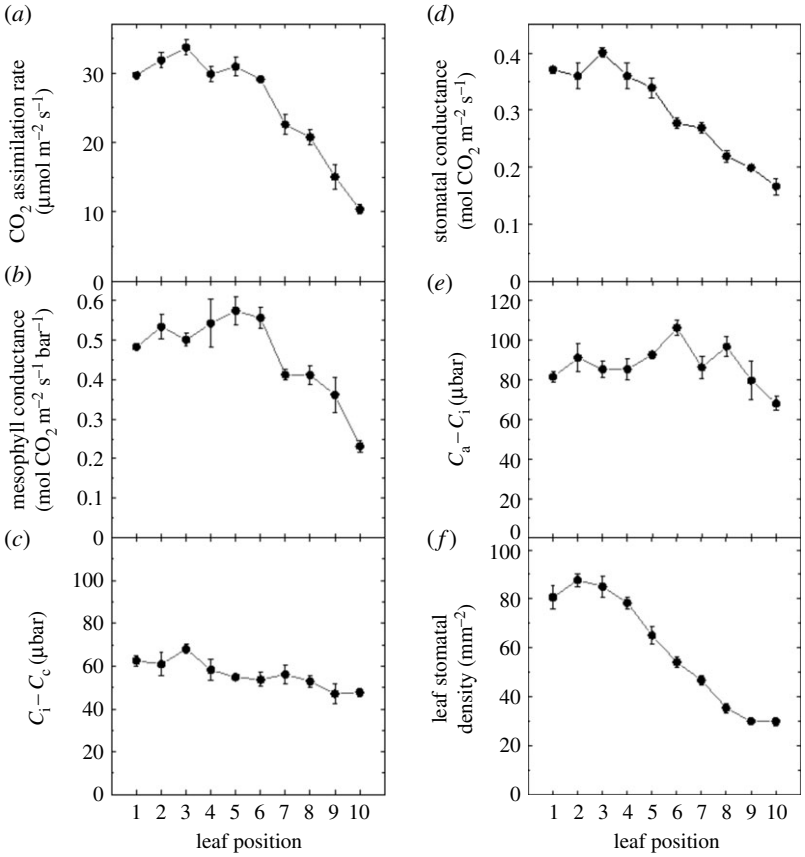

Figure 5. Variation in CO_2 assimilation rate (*a*), mesophyll conductance (*b*), $C_i - C_c$ (*c*), stomatal conductance (*d*), $C_a - C_i$ (*e*) and abaxial stomatal number per leaf area (*f*) with leaf position in the canopy (figure 3). Gas exchange measurements were made at an irradiance of 1500 µmol m^{-2} s^{-1}, ambient CO_2 of 380 µbar, 2% O_2 and a leaf temperature of 25°C. Gas exchange measurements were made concurrently with measurements of carbon isotope discrimination using tunable diode laser spectroscopy for the calculation of mesophyll conductance (see Materials and methods), $n = 4$ plants. Raw data are given in the electronic supplementary material, Data File S2.

microscope (Leica Microsystems) and used to measure leaf thickness and mesophyll layer thickness. For scanning electron microscopy, ultrathin sections were mounted onto pieces of silicon wafer and post-stained with aqueous uranyl acetate followed by lead citrate for 10 min each prior to imaging under a Zeiss UltraPlus field emission scanning electron microscope at 2 kV. Scanning electron micrographs were used to measure mesophyll cell wall thickness, chloroplast length, chloroplast thickness, the surface area of mesophyll cells exposed to intercellular airspace per unit leaf area (S_{mes}) and surface area of chloroplasts exposed to intercellular airspace per unit leaf area (S_c). Electron micrograph measurements were performed according to Evans *et al*. [13] using at least 600 µm leaf surface length for each leaf position per plant. Stomatal density was measured from positives made with nail polish from hydrophilic vinyl polysiloxane impressions of the abaxial surface of the leaf area measured by gas exchange, and viewed under a Leica confocal microscope and Leica DC500 camera. All measurements were made using ImageJ software (National Institutes of Health) and a Wacom Cintiq graphics tablet (Wacom Technology).

2.5. Statistical analysis

Statistical analyses were performed using Student's *t*-test for figure 2, and all other data using one-way analysis of variance. Means comparison was made at 0.05 significance level using the Tukey test (OriginPro 2020, OriginLab Corporation).

3. Results

3.1. Changes in leaf physiology over time

To understand how mesophyll conductance, g_m, is influenced by leaf ageing, leaf physiology traits were repeatedly measured in a tobacco leaf over four weeks of growth. CO_2 assimilation rate, A, stomatal conductance, g_s, and g_m all decreased in the ageing tobacco leaf over time (figure 2). The drawdown of CO_2 into the chloroplast ($C_i - C_c$), however, was not significantly changed over the four weeks of measurements. The drawdown of CO_2 into the sub-stomatal cavity ($C_a - C_i$) increased between 6 and 8-week-old leaves, but was not significantly different overall between the 6-week and 9-week measurements (figure 2). Raw data for figure 2 are given in the electronic supplementary material, Data File S1.

3.2. The effect of canopy position on leaf anatomy and physiology

The effect of leaf canopy position was further investigated in 9-week-old tobacco plants with 10 leaves through measurement of physiological and anatomical traits. To determine whether there is a direct correlation between the leaf anatomy and g_m, structural and ultrastructural analyses were performed using the leaf tissue from the same area as used for physiological measurement. Light micrographs of transverse leaf sections showed that leaf thickness and mesophyll cell layer thickness increase as the leaf matures (figures 3 and 4*b*,*c*). Surprisingly this was not accompanied by a significant increase in leaf mass per area (LMA, figure 4*a*), which varied from 24.8 ± 0.6 g m^{-2} in leaf 1 to 32.1 ± 2.1 g m^{-2} in leaf 9. Measurements performed using electron micrographs of the same leaf sections revealed that chloroplast surface area exposed to the intercellular airspace per unit leaf area (S_c, figure 4*d*) and mesophyll surface area exposed to the

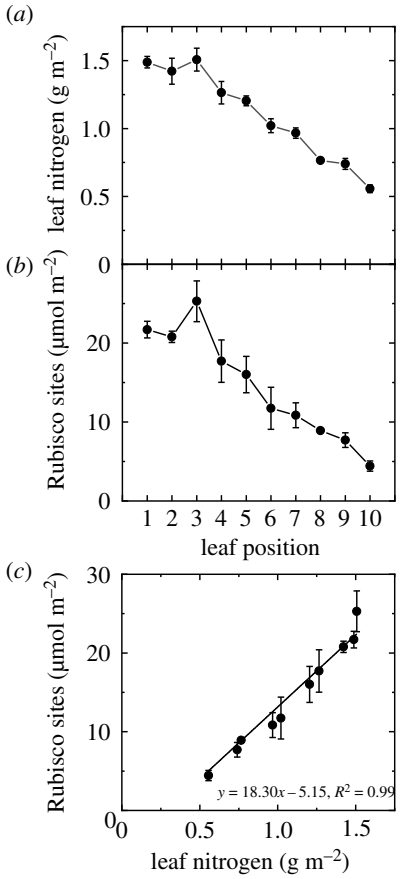

Figure 6. Variation in leaf nitrogen (*a*) and Rubisco site content (*b*) with leaf position in the canopy (figure 3). The relationship between Rubisco sites and leaf nitrogen is shown in (*c*), $n = 4$ plants. Raw data are given in the electronic supplementary material, Data File S2.

intercellular airspace per unit leaf area (S_{mes}, figure 4*e*) decrease after leaf position 6. Reduced values of S_c and S_{mes} in leaf positions 7–10 (figure 4*d*,*e*) resulted in decreasing values of chloroplast cover of the exposed mesophyll cells, S_c/S_{mes}, in the same leaf positions (figure 4*f*). Significant statistical differences of means at the 5% level ($p < 0.05$) are summarized in table 1 for all parameters shown in figures 4–6 and 8, and the raw data are given in the electronic supplementary material, Data File S2.

CO_2 assimilation rate, A, decreased from maximal values in leaves at the top of the leaf canopy down to leaves at the base of the canopy, particularly from leaf 7–10 (figure 5*a*,*b*, table 1). Mesophyll conductance decreased strongly from leaf 6 onwards. Stomatal conductance also showed a similar decrease in the canopy (figure 5*d*). The variation in the drawdown of CO_2 from the atmosphere into the sub-stomatal cavity ($C_a - C_i$, figure 5*e*) and from the sub-stomatal cavity into the chloroplasts ($C_i - C_c$, figure 5*c*) was less dynamic, but significant differences were still apparent between leaves at the top and bottom of the canopy (table 1). The number of stomata per mm^2 leaf area (stomatal density, figure 5*f*) decreased moving down the canopy due to the overall expansion of the pavement cells on the leaf surface as the leaves aged (electronic supplementary material, figure S1). There was a strong correlation between stomatal conductance and stomatal density ($y = 0.0034x + 0.092$, $R^2 = 0.95$).

Leaf nitrogen (N) content was highest in the youngest leaves at the top of the canopy, and steadily declined through the lower leaf positions (figure 6*a*). Rubisco content also decreased down the canopy (figure 6*b*) and was found to be very closely correlated to leaf nitrogen content (figure 6*c*, $R^2 = 0.99$). There was a strong linear relationship between g_m and A ($y = 0.0126x + 0.142$, $R^2 = 0.71$, electronic supplementary material, figure S2). However, the relationships between g_m and Rubisco content or leaf N were best fitted with a second-order polynomial (electronic supplementary material, figure S2) as were the relationships between A and Rubisco content and leaf N (electronic supplementary material, figure S3). This shows that A per Rubisco or leaf N was less in leaves at the top of the canopy than in older leaves further down the canopy.

Electron micrographs also allowed measurements of mesophyll chloroplast thickness, mesophyll chloroplast length and mesophyll cell wall thickness in leaf positions 1–10 (figure 7). Results showed a decrease in mesophyll chloroplast thickness (figure 8*a*), an increase in mesophyll chloroplast length (figure 8*b*) and thickening of mesophyll cell walls (figure 8*c*) as the leaf matures. Measurements and calculations also revealed that the thicker mesophyll cell wall in older leaves (figure 8*c*) was directly proportional to the mesophyll resistance ($r_m = 1/g_m$, figure 9*a*). This resistance ranged from 1.5 in young leaves to 4 m^2 s bar mol^{-1} in lower canopy leaves and the inverse g_m ranged from 0.7 to 0.2 mol m^{-2} s^{-1} bar^{-1}. There was only a weak correlation between mesophyll conductance and the chloroplast surface area exposed to intercellular airspace (S_c, figure 9*b*).

4. Discussion

4.1. Mesophyll conductance correlates with CO_2 assimilation rate

CO_2 assimilation rate, A, and mesophyll conductance, g_m, both decreased as leaves moved lower in the tobacco canopy, with a strong linear correlation between A and g_m reflected in a constant difference in CO_2 partial pressure between intercellular airspace and the chloroplasts ($C_i - C_c$) across leaf positions (figure 5, and electronic supplementary material, figure S2). Strong correlations between A and g_m have previously been observed with leaf development or ageing [14,16,19,20,28,29]. In a study with transgenic tobacco plants where Rubisco content was reduced, the correlation did not hold and A declined more than g_m [13]. This indicates that it is not a mechanistic relationship between A and g_m. Both A and g_m showed curvilinear responses to Rubisco and leaf nitrogen (electronic supplementary material, figures S2 and S3) suggesting that the link between A and g_m is the most useful for the incorporation of g_m in canopy photosynthesis and crop models [10,30–32].

4.2. Relationship between CO_2 assimilation rate and Rubisco and leaf N content

Rubisco accounts for around 40% of soluble protein in a leaf and around 20% of leaf nitrogen (N) investment in C_3 species [33]. We saw a very close correlation between leaf N and Rubisco, suggesting that the proportional investment in Rubisco across leaves remained constant across the canopy. We also observed curvilinear relationships between A and Rubisco content or leaf N (electronic supplementary material, figure S3) with young leaves having a lower Rubisco and leaf N use efficiency. Curvilinear responses have been observed in the past and two explanations have been put forward [34].

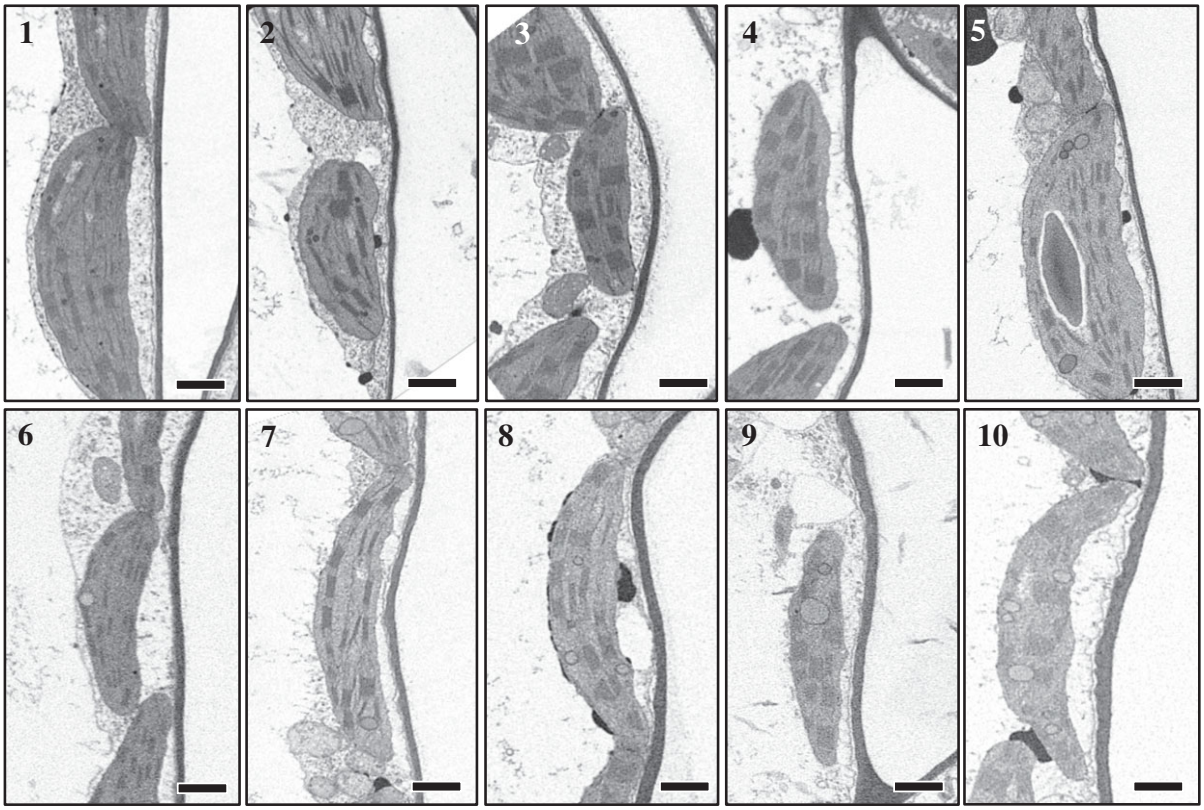

Figure 7. Electron micrographs of transverse sections of resin-embedded leaf tissue collected from leaf position 1 to 10 of 9-week-old tobacco plant showing variation in mesophyll cell wall thickness (see figure 8*c* for measured values). Bars = 1 µm.

The first one suggests it could be a CO_2 diffusion limitation, but since we know that there has been no increase in either $C_a - C_i$ or $C_i - C_c$ we can rule out a CO_2 diffusion limitation. The second reason given by Evans [34] is that with increasing leaf N the chlorophyll and electron transport capacity increase and to reach light saturation requires progressively higher irradiances. Since we measured at the same irradiance the maximal rate of the high nitrogen leaf is underestimated. We only made measurements of A at one irradiance and this could be further investigated.

4.3. Linking mesophyll conductance and leaf anatomy

Figures 3, 4 and 7–9 highlight the large anatomical changes that occur during leaf development. There was a doubling of leaf thickness but this did not result in significant changes in leaf mass per area (LMA) despite the increase in cell wall thickness. In an across species comparison higher LMA has been associated with decreased g_m and an increase in the percentage that cell wall mass contributes to LMA [35]. However, tobacco, as a herbaceous crop species, has a low LMA compared to species tested in that study, and cell wall mass is expected to contribute no more than 10–15% of LMA (figure 3; [35]). It is therefore not surprising that we saw little change in LMA despite an increase in cell wall thickness and reduction in g_m. We conclude that increased airspace and cell volume account for these changes.

To facilitate CO_2 diffusion, chloroplasts line mesophyll cell walls adjacent to intercellular airspace. Anatomical parameters such as S_c and S_{mes} are similar to those measured in glasshouse grown tobacco in previous studies [13] providing a chloroplast surface area 15 times greater than the projected leaf area. As chloroplasts cover 80% or more of mesophyll cell walls adjacent to intercellular airspace, there is room for only small improvements of g_m by increasing S_c/S_{mes}. However, S_c/S_{mes} has been shown to be less in low light conditions and under stress in *Populus tremula*, and can vary with growth conditions [14]. Compared to the rapid decline in CO_2 assimilation rate with leaf position, S_c remained unchanged up to leaf position 7 and is therefore not the driver for the reduction in CO_2 assimilation rates or g_m (figure 9*b*). Other studies that have also compared changes in A, g_m and S_c with leaf age variation also reported the poor correlation between g_m and S_c under these conditions [16,19,20].

As depicted in figure 1 CO_2 has to diffuse from intercellular airspace across the cell wall, the plasma membrane, cytosol, chloroplast envelope and the chloroplast stroma. Of these obstacles in the diffusion path, cell wall thickness and chloroplast shape are measurable components. We observed a continuous increase in cell wall thickness from the top to the bottom of the canopy and observed a strong inverse correlation between g_m and cell wall thickness (figure 9*a*). This highlights the important contribution of cell wall thickness in determining g_m and is in line with previous studies [12,15,36,37]. Tobacco like many crop species has relatively thin cell walls [36]; however, it is not just the physical dimension but also cell wall composition that matters and we know little about this at present (see [38] for a review of current knowledge). If we extrapolate to zero cell wall thickness we see a resistance of 0.6 m^2 s bar mol^{-1} (figure 9*a*) equating to a mesophyll conductance of 1.6 mol m^{-2} s^{-1} bar^{-1}. While we cannot accurately measure the resistance derived from plant membranes, we know that membrane composition (such as the presence of channels for facilitating CO_2 transfer) together with CO_2 diffusion through the liquid phases also contributes to mesophyll resistance [39]. Nevertheless, our results highlight that thinner cell walls, if structurally possible, could be of benefit to improve mesophyll conductance.

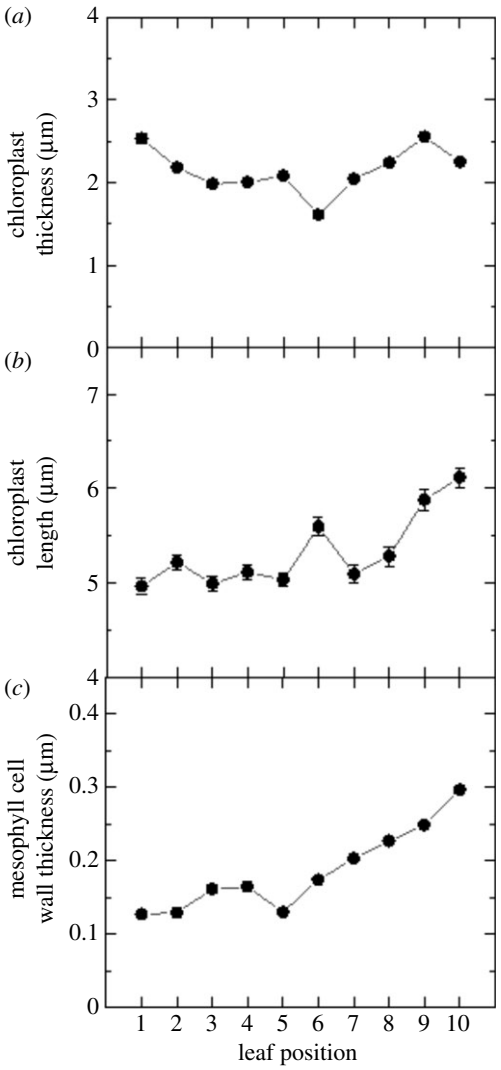

Figure 8. Variation in chloroplast thickness (*a*), chloroplast length (*b*) and mesophyll cell wall thickness (*c*) with leaf position in the canopy (figure 3), $n = 3$ plants. Raw data are given in the electronic supplementary material, Data File S2.

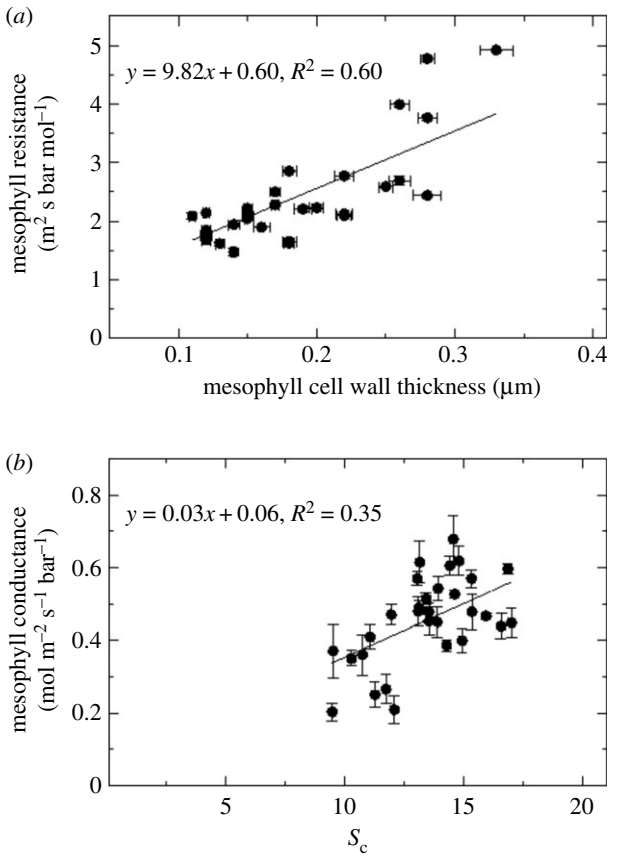

Figure 9. The relationship between mesophyll resistance ($r_m = 1/g_m$) and mesophyll cell wall thickness (*a*) and between mesophyll conductance and S_c, the chloroplast surface area exposed to intercellular airspace per unit leaf area (*b*). Each data point corresponds to an average value per leaf from three plants. Raw data are given in the electronic supplementary material, Data File S2.

5. Conclusion

We combined gas exchange and anatomical measurements to assess how CO_2 assimilation rate, A, and mesophyll conductance, g_m, decreased as leaves aged and whether we could link decreases in g_m with leaf anatomy. Surprisingly we observed a decrease in the chloroplast surface area exposed to the intercellular airspace per unit leaf area, S_c, only low in the canopy whereas there was a gradual increase in cell wall thickness and an inverse correlation between g_m and cell wall thickness. We conclude that reduced g_m of older leaves lower in the canopy was associated with a reduction in S_c and a thickening of mesophyll cell walls. The relationship between A and g_m, however, is the most useful for the incorporation of g_m in canopy photosynthesis and crop models. In crop species where mesophyll cell chloroplast cover is high, increasing the conductance across the chloroplast interface is the major challenge for improvements in mesophyll conductance, which will enhance photosynthetic capacity and ultimately increase crop yields.

Data accessibility. Raw data are available in the electronic supplementary materials of this article.

Authors' contributions. V.C.C. designed and conducted physiology and biochemistry experiments, analysed data and wrote the manuscript; F.R.D. conducted anatomy experiments, analysed data and edited the manuscript; S.v.C. planned the study, contributed resources and facilities, analysed data and wrote the manuscript.

Competing interests. We declare we have no competing interests.

Funding. This research was supported by a sub-award from the University of Illinois as part of the Realizing Increased Photosynthetic Efficiency (RIPE) project, funded by the Bill & Melinda Gates Foundation to V.C.C. and S.v.C. and the Australian Research Council Centre of Excellence for Translational Photosynthesis (CE1401000015) for S.v.C. and F.R.D.

Acknowledgements. We thank the Centre for Advanced Microscopy and Microscopy Australia for providing the facility and Joanne Lee for technical assistance. We also thank Tenzin Norzin for her contributions to data collection in an early iteration of this experiment.

References

1. von Caemmerer S, Evans JR. 1991 Determination of the average partial pressure of CO_2 in chloroplast from leaves of several C_3 plants. *Aust. J. Plant Physiol.* **18**, 287–305. (doi:10.1071/PP9910287)

2. Flexas J *et al.* 2012 Mesophyll diffusion conductance to CO_2: an unappreciated central player in

photosynthesis. *Plant Sci.* **193**, 70–84. (doi:10.1016/j.plantsci.2012.05.009)

3. Ray DK, Mueller ND, West PC, Foley JA. 2013 Yield trends are insufficient to double global crop production by 2050. *PLoS ONE* **8**, e66428. (doi:10.1371/journal.pone.0066428)
4. von Caemmerer S, Evans JR. 2010 Enhancing C_3 photosynthesis. *Plant Physiol.* **154**, 589–592. (doi:10.1104/pp.110.160952)
5. Sharkey TD. 2012 Mesophyll conductance: constraint on carbon acquisition by C_3 plants. *Plant Cell Environ.* **35**, 1881–1883. (doi:10.1111/pce.12012)
6. Bailey-Serres J, Parker JE, Ainsworth EA, Oldroyd GED, Schroeder JI. 2019 Genetic strategies for improving crop yields. *Nature* **575**, 109–118. (doi:10.1038/s41586-019-1679-0)
7. Adachi S *et al.* 2013 The mesophyll anatomy enhancing CO_2 diffusion is a key trait for improving rice photosynthesis. *J. Exp. Bot.* **64**, 1061–1072. (doi:10.1093/Jxb/Ers382)
8. Flexas J *et al.* 2013 Diffusional conductances to CO_2 as a target for increasing photosynthesis and photosynthetic water-use efficiency. *Photosynth. Res.* **117**, 45–59. (doi:10.1007/s11120-013-9844-z)
9. Zhu X-G, Ort DR, Parry M, von Caemmerer S. 2020 A wish list for synthetic biology in photosynthesis research. *J. Exp. Bot.* **71**, 2219–2225. (doi:10.1093/jxb/eraa075)
10. Yin X, Struik PC. 2017 Can increased leaf photosynthesis be converted into higher crop mass production? A simulation study for rice using the crop model GECROS. *J. Exp. Bot.* **68**, 2345–2360. (doi:10.1093/jxb/erx1085)
11. Cousins AB, Mullendore DL, Sonawane BV. 2020 Recent developments in mesophyll conductance in C3, C4, and crassulacean acid metabolism plants. *Plant J.* **101**, 816–830. (doi:10.1111/tpj.14664)
12. Evans JR, Kaldenhoff R, Genty B, Terashima I. 2009 Resistances along the CO_2 diffusion pathway inside leaves. *J. Exp. Bot.* **60**, 2235–2248. (doi:10.1093/jxb/erp117)
13. Evans JR, von Caemmerer S, Setchell BA, Hudson GS. 1994 The relationship between CO_2 transfer conductance and leaf anatomy in transgenic tobacco with a reduced content of Rubisco. *Aust. J. Plant Physiol.* **21**, 475–495. (doi:10.1071/PP9940475)
14. Tosens T, Niinemets U, Vislap V, Eichelmann H, Diez PC. 2012 Developmental changes in mesophyll diffusion conductance and photosynthetic capacity under different light and water availabilities in *Populus tremula*: how structure constrains function. *Plant Cell Environ.* **35**, 839–856. (doi:10.1111/j.1365-3040.2011.02457.x)
15. Terashima I, Hanba YT, Tholen D, Niinemets U. 2011 Leaf functional anatomy in relation to photosynthesis. *Plant Physiol.* **155**, 108–116. (doi:10.1104/pp.110.165472)
16. Hanba YT, Miyazawa SI, Kogami H, Terashima I. 2001 Effects of leaf age on internal CO_2 transfer conductance and photosynthesis in tree species having different types of shoot phenology. *Aust. J. Plant Physiol.* **28**, 1075–1084. (doi:10.1071/PP00102)
17. Niinemets U, Cescatti A, Rodeghiero M, Tosens T. 2005 Leaf internal diffusion conductance limits photosynthesis more strongly in older leaves of Mediterranean evergreen broad-leaved species. *Plant Cell Environ.* **28**, 1552–1566. (doi:10.1111/j.1365-3040.2005.01392.x)
18. Marchi S, Tognetti R, Minnocci A, Borghi M, Sebastiani L. 2008 Variation in mesophyll anatomy and photosynthetic capacity during leaf development in a deciduous mesophyte fruit tree (*Prunus persica*) and an evergreen sclerophyllous Mediterranean shrub (*Olea europaea*). *Trees Struct. Funct.* **22**, 559–571. (doi:10.1007/s00468-008-0216-9)
19. Barbour MM, Evans JR, Simonin KA, von Caemmerer S. 2016 Online CO_2 and H_2O oxygen isotope fractionation allows estimation of mesophyll conductance in C_4 plants, and reveals that mesophyll conductance decreases as leaves age in both C_4 and C_3 plants. *New Phytol.* **210**, 875–889. (doi:10.1111/nph.13830)
20. Evans JR, Vellen L. 1996 Wheat cultivars differ in transpiration efficiency and CO_2 diffusion inside their leaves. In *Crop research in Asia: achievements and perspective* (eds R Ishii, T Horie), pp. 326–329. Tokyo, Japan: Asian Crop Science Association.
21. Scartazza A, Lauteri M, Guido MC, Brugnoli E. 1998 Carbon isotope discrimination in leaf and stem sugars, water-use efficiency and mesophyll conductance during different developmental stages in rice subjected to drought. *Funct. Plant Biol.* **25**, 489–498. (doi:10.1071/PP98017)
22. Tazoe Y, von Caemmerer S, Estavillo GM, Evans JR. 2011 Using tunable diode laser spectroscopy to measure carbon isotope discrimination and mesophyll conductance to CO_2 diffusion dynamically at different CO_2 concentrations. *Plant Cell Environ.* **34**, 580–591. (doi:10.1111/j.1365-3040.2010.02264.x)
23. von Caemmerer S, Farquhar GD. 1981 Some relationships between the biochemistry of photosynthesis and the gas exchange of leaves. *Planta* **153**, 376–387. (doi:10.1007/BF00384257)
24. Evans JR, Sharkey TD, Berry JA, Farquhar GD. 1986 Carbon isotope discrimination measured concurrently with gas exchange to investigate CO_2 diffusion in leaves of higher plants. *Aust. J. Plant Physiol.* **13**, 281–292. (doi:10.1071/PP9860281)
25. Evans JR, von Caemmerer S. 2013 Temperature response of carbon isotope discrimination and mesophyll conductance in tobacco. *Plant Cell Environ.* **36**, 745–756. (doi:10.1111/j.1365-3040.2012.02591.x)
26. Ruuska S, Andrews TJ, Badger MR, Hudson GS, Laisk A, Price GD, von Caemmerer S. 1998 The interplay between limiting processes in C_3 photosynthesis studied by rapid-response gas exchange using transgenic tobacco impaired in photosynthesis. *Aust. J. Plant Physiol.* **25**, 859–870. (doi:10.1071/PP98079)
27. Danila FR, Quick WP, White RG, Furbank RT, von Caemmerer S. 2016 The metabolite pathway between bundle sheath and mesophyll: quantification of plasmodesmata in leaves of C_3 and C_4 monocots. *Plant Cell* **28**, 1461–1471. (doi:10.1105/tpc.16.00155)
28. Loreto F, Di Marco G, Tricoli D, Sharkey T. 1994 Measurements of mesophyll conductance, photosynthetic electron transport and alternative electron sinks of field grown wheat leaves. *Photosynth. Res.* **41**, 397–403. (doi:10.1007/BF02183042)
29. Evans JR, von Caemmerer S. 1996 Carbon dioxide diffusion inside leaves. *Plant Physiol.* **110**, 339–346. (doi:10.1104/pp.110.2.339)
30. Wu A, Hammer GL, Doherty A, von Caemmerer S, Farquhar GD. 2019 Quantifying impacts of enhancing photosynthesis on crop yield. *Nat. Plants* **5**, 380–388. (doi:10.1038/s41477-019-0398-8)
31. Wu A, Doherty A, Farquhar GD, Hammer GL. 2018 Simulating daily field crop canopy photosynthesis: an integrated software package. *Funct. Plant Biol.* **45**, 362–377. (doi:10.1071/FP17225)
32. Song Q, Chen D, Long SP, Zhu X-G. 2017 A user-friendly means to scale from the biochemistry of photosynthesis to whole crop canopies and production in time and space – development of Java WIMOVAC. *Plant. Cell Environ.* **40**, 51–55. (doi:10.1111/pce.12816)
33. Evans JR, Clarke VC. 2018 The nitrogen cost of photosynthesis. *J. Exp. Bot.* **70**, 7–15. (doi:10.1093/jxb/ery366)
34. Evans JR. 1989 Photosynthesis and nitrogen relationships in leaves of C_3 plants. *Oecologia* **78**, 9–19. (doi:10.1007/BF00377192)
35. Onoda Y, Wright IJ, Evans JR, Hikosaka K, Kitajima K, Niinemets Ü, Poorter H, Tosens T, Westoby M. 2017 Physiological and structural tradeoffs underlying the leaf economics spectrum. *New Phytol.* **214**, 1447–1463. (doi:10.1111/nph.14496)
36. Gago J, Carriquí M, Nadal M, Clemente-Moreno MJ, Coopman RE, Fernie AR, Flexas J. 2019 Photosynthesis optimized across land plant phylogeny. *Trends Plant Sci.* **24**, 947–958. (doi:10.1016/j.tplants.2019.07.002)
37. Sugiura D, Terashima I, Evans JR. 2020 A decrease in mesophyll conductance by cell wall thickening contributes to photosynthetic down-regulation. *Plant Physiol.* **183**, 1600–1611. (doi:10.1104/pp.20.00328)
38. Gago J *et al.* 2020 The photosynthesis game is in the 'inter-play': mechanisms underlying CO_2 diffusion in leaves. *Environ. Exp. Bot.* **178**, 104174. (doi:10.1016/j.envexpbot.2020.104174)
39. Evans JR. 2020 Mesophyll conductance: walls, membranes and spatial complexity. *New Phytol.* **229**, 1864–1876. (doi:10.1111/nph.16968)